Automated follow-up of GRB afterglows with the Palomar 60-inch telescope: the complete 13-year sample

Aleksandra Bochenek[1], Daniel A. Perley[1], S. Bradley Cenko[2]

[1]Astrophysics Research Institute, Liverpool John Moores University, [2]NASA Goddard Space Flight Centre

INTRODUCTION

The **Palomar 60-inch** (1.5m) telescope, **P60**, conducted a fully automated optical GRB follow-up campaign **between 2004 and 2016**. This resulted in **88 early observations** (within one hour of trigger) of Swift GRBs, **minimizing selection biases** and **accurately reflecting Swift's sensitivity**. With **55 afterglow detections**, this sample is a valuable tool for investigating the full GRB population.

This poster presents the initial analysis of the full sample, following after Cenko+2009, who characterised the sample up to March 2008.

The follow-up programme was characterised by quick response time to GRB triggers and depth of observations:

- **response to trigger: ~ 3 min**
- **typical depth**: **r ~ 20 mag** in a single 60 s exposure
- imaging with GRBCam camera, typically in the **g, r, i** and **z filters**.

88 'early' observations of Swift GRBs → 55 afterglows - 63% detection rate → 40 afterglows with redshifts

P60 LIGHT CURVES

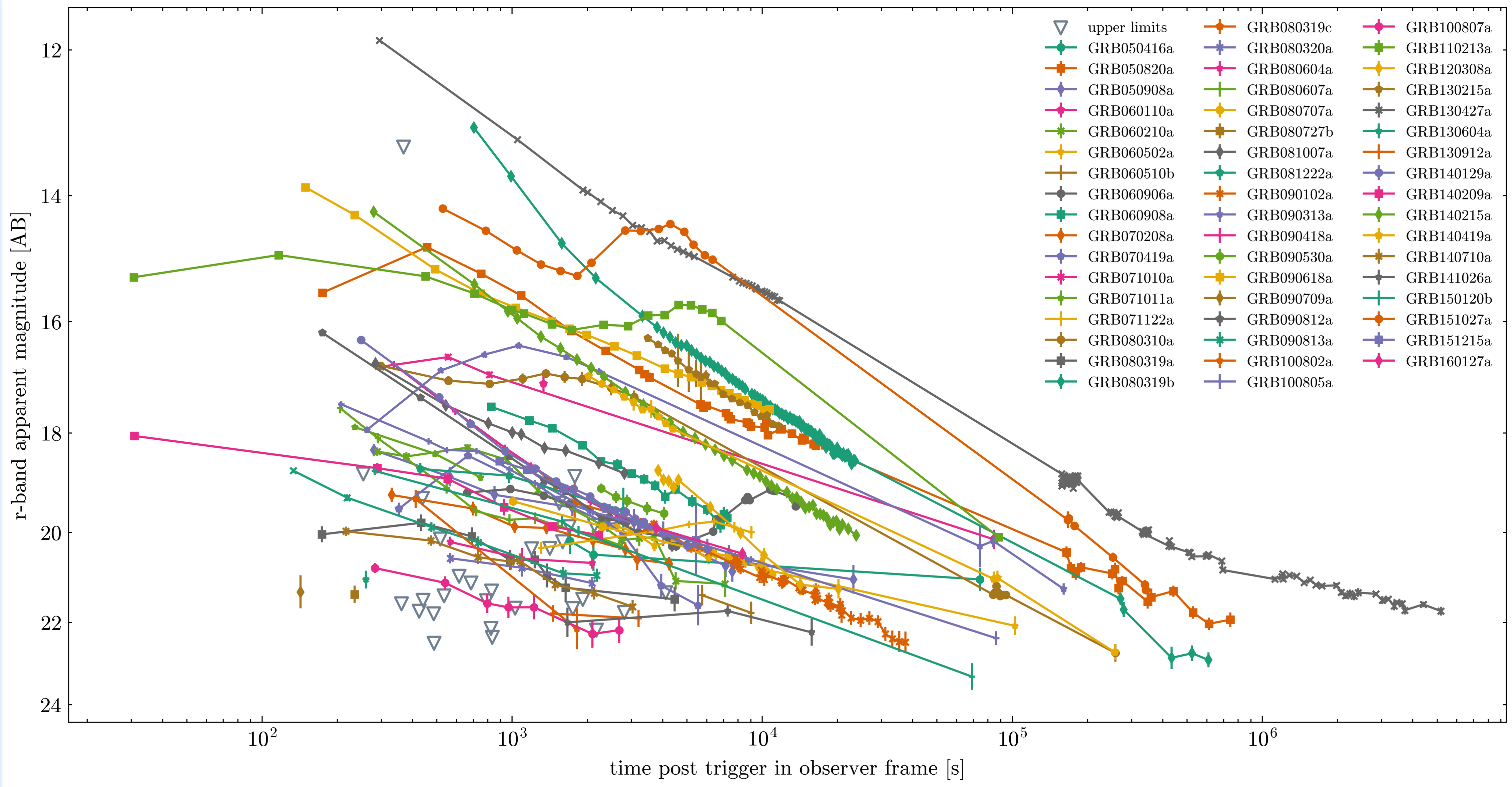

Figure 1. The P60 early afterglow sample of apparent r-band light curves for detected events, without extinction correction. Observations pre-2009 are in Cousins R filter, and later are in SDSS-r The plot does not include several GRBs yet such as GRB050713a and GRB071003a, due to the need for more complicated background subtraction. Grey upper limit markers are each for a different objects. n some cases, early observations captured afterglow rise, while certain events (e.g., GRB060906a) show atypical light curves.

The project began by identifying **early P60 observations** via cross-matching GRBCam data (IRSA) with Swift triggers. Photometry on each object was done relative to Pan-STARRS, or, in a few cases with declinations lower than -30 deg, to the SkyMapper catalogue.

Part of the P60 sample, up to March 2008, is already published (Cenko+2009). Therefore, **an important part of this project was ensuring agreement between this project results' and the already published sample**. Minor photometric offsets were found in a few cases, while the light curve shapes remained unchanged, likely due to improved calibration star access.

BASIC CHARACTERISTICS

Each afterglow was **corrected for Milky Way dust extinction**, and those **with available redshifts were also k-corrected**. The corrected flux was used to derive the decay index α and spectral index β, fitting the full dataset on a plane with a logged equation based on the $\mathbf{F} \propto \mathbf{t}^{\alpha}\mathbf{\nu}^{\beta}$ relationship.

Since the strength of the sample is the availability of early data, **α and β were calculated at t = 1000 s in the rest frame**. $\alpha_{\mathrm{mean}} = -0.74$ aligns with other results for afterglow in early phases in their evolution (e.g., Oates+2009, Nysewander+2009). However, $\beta_{\mathrm{mean}} = -1.47$ deviates from theoretical expectations of $\beta = -0.6$ (Sari+1998) and previous Swift results ($\beta = -0.66$; Kann+2010). This discrepancy potentially arises from the P60 sample not being corrected for host extinction, though the steeper β is consistent with the results from Melandri+2008 automatically followed-up sample, suggesting an impact from early 'dark' afterglows.

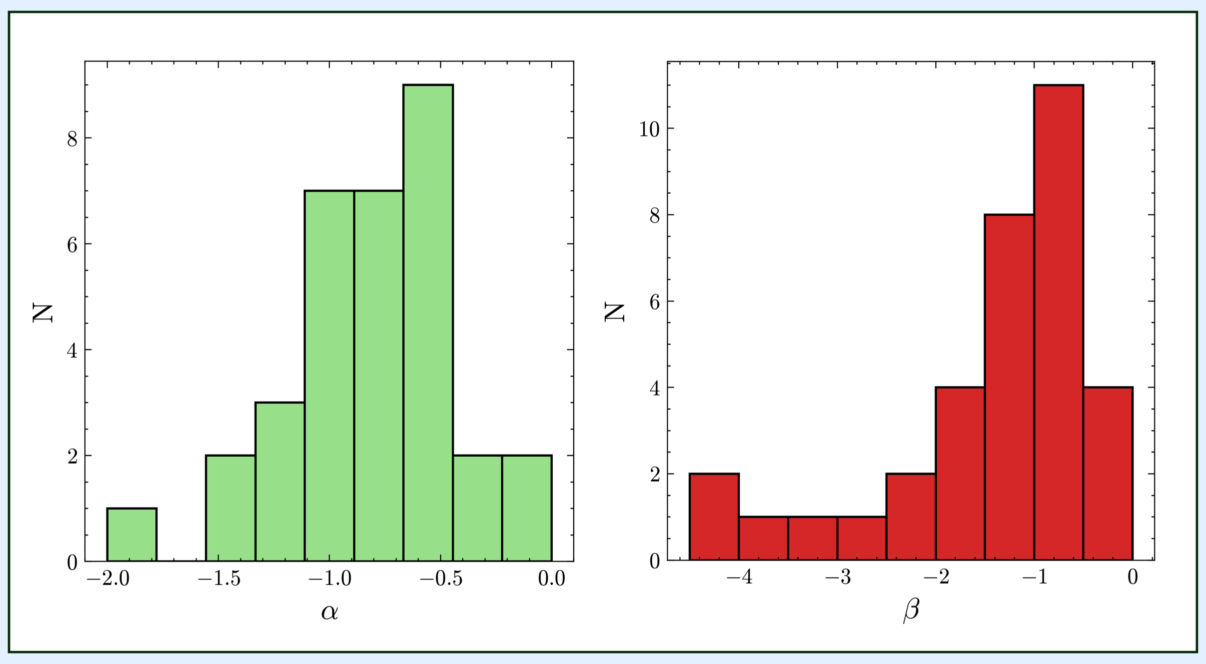

Figure 2. Distribution plots showing, from the left, decay index distribution of P60 afterglows at t = 1000 s in rest frame, with mean $\alpha = -0.74$ and σ = 0.57. The spectral index distribution has a mean $\beta = -1.47$, median $= -1.12$, and $\sigma = 1.07$, with a tail towards steeper/redder values.

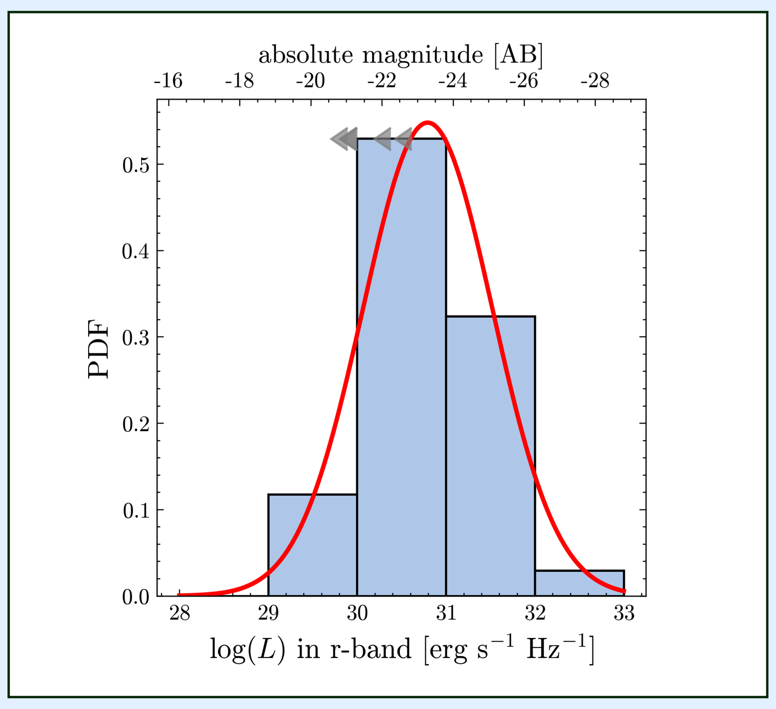

Figure 3. Distribution of r-band luminosities at t = 1000 s, and a fitted normal distribution with $\log(L)_{\mathrm{mean}}$ = (30.79 ± 0.73 dex) erg $s^{-1}Hz^{-1}$. The upper limits are events that are P60 non-detections, but have known redshifts.

Each object's luminosity at t = 1000 s was computed in the corresponding r-filter, producing a centrally peaked distribution. A normal distribution fit peaks at log(L) = (30.79 ± 0.73) erg $s^{-1}Hz^{-1}$, slightly higher than log(L) ~ 30.10 erg $s^{-1}Hz^{-1}$ of Kann+ 2011 for Type II GRBs, and comparable than Melandri+2008 at ~ (30.64 ± 0.14) erg $s^{-1}Hz^{-1}$, if both were transformed to common filter and time.

FURTHER WORK - redback

To recover other qualities of the P60 afterglows, I began using **redback** (Sarin+24) **to fit tophat and gaussian afterglowpy models** (Ryan+2020), wrapped with bilby (Ashton+2019) to P60 data. The fits make use of XRT data and, whenever available, radio data. Figure 3 shows a gaussian jet fit for GRB090618.

The numerical models in redback will be used to constrain GRB characteristics such as jet opening angles, Lorentz factors, their peak energies or energy ranges, etc. Bringing together those models with observations will allow to make a prediction about the expected rates of relativistic events.

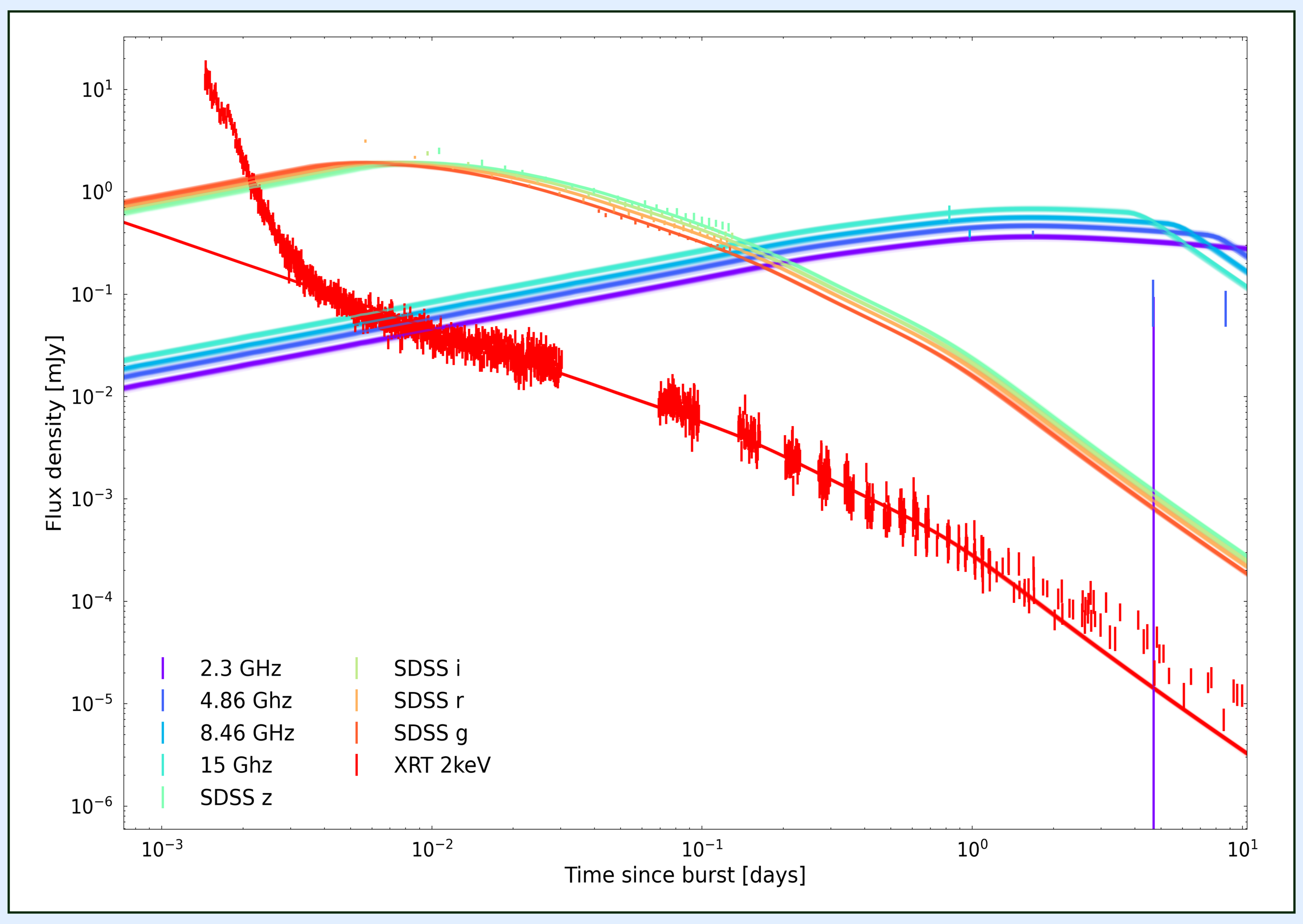

Figure 3. Fit to GRB090618a optical, radio, and X-ray data of a gaussian jet model from afterglowpy, implemented in redback. The optical data is from P60, the radio observations from Cano+2011, and XRT observations from Schady+2009; Evans+2009; Beardmore & Schady+2009.

CONCLUSIONS

The survey aimed to present an **unbiased sample of Swift GRB afterglows, constraining their characteristics and providing insight into the overall GRB population**. Initial results are **consistent with previous studies** but reveal a **steeper, redder spectral index** than expected, possibly reflecting the impact of a **dustier GRB population** than the currently measured one. A lot of work remains to be done on the sample, including characterizing the sample at different timescales, or comparison with X-ray flux and spectral index. The dataset combined with observations from other facilities and numerical modelling, will provide **a deeper understanding of GRB jet properties and occurrence rates**.

Acknowledgements

All data in this survey has been gathered through a project led by Dr S. Bradley Cenko and was made available to me, for which I am very grateful. The Palomar Observatory is operated by the California Institute of Technology, and I would also like to thank the Palomar Observatory staff and the GRB follow-up team there.

The P60 telescope is located on Palomar Mountain, part of the traditional homelands of the Pauma People.

Bibliography

Cenko S. B. et al. (2006) *The Automated Palomar 60 Inch Telescope*, PASP 118
Cenko S. B. et al. (2008) *Dark Bursts in the Swift Era: the Palomar 60 inch Swift Early Optical Afterglow Catalog*, ApJ, 693
Gehrels, N. et al. (2009) *Gamma-Ray Bursts in the Swift Era*, ARAA, 47
Melandri A. et al. (2008) *The Early-Time Optical Properties of Gamma-Ray Burst Afterglows*, ApJ, 686
Akerlof C. W. & Swan H. (2007) *An Estimation of the Gamma-Ray Burst Afterglow Apparent Optical Brightness Distribution Function*, Apj, 671
Kann D. A. et al. (2010) *The Afterglows of Swift-era Gamma-ray Bursts. I. Comparing pre-Swift and Swift-era Long/Soft* (Type II) GRB Optical Afterglows, ApJ 720
Kann D. A. et al. (2011) *The Afterglows of Swift-era Gamma-Ray Bursts. II. Type I GRB versus Type II GRB Optical Afterglows*, ApJ, 734
Sarin N. et al. (2024) *REDBACK: a Bayesian inference software package for electromagnetic transients,* MNRAS 351